Influence of the 17 August 1999 Izmit Earthquake on Seismic Hazards in Istanbul

Tom Parsons[1], (tparsons@usgs.gov)
Aykut Barka[2], (barka@itu.edu.tr)
Shinji Toda[3], (s-toda@aist.go.jp)
Ross S. Stein[1], (rstein@usgs.gov)
James H. Dieterich[1], (jdieterich@usgs.gov)

[1] US Geological Survey, 345 Middlefield Rd – MS 977, Menlo Park, CA 94025
[2] Istanbul Technical University, Istanbul, Turkey
[3] Earthquake Research Institute, University of Tokyo, Japan

Abstract

We calculate the probability of strong shaking in Istanbul—an urban center of 10 million people—from the description of earthquakes on the North Anatolian fault system in the Marmara Sea during the past 500 years, and test the resulting catalog against the frequency of damage in Istanbul during the preceding millennium. Departing from current practice, we include the time-dependent effect of stress transferred by the 1999 moment magnitude M=7.4 Izmit earthquake to faults nearer to Istanbul. We find a 62±15% probability (one standard deviation) of strong shaking during the next 30 years and 32±12% during the next decade.

Parsons, T., A. Barka, et al. (2000). Influence of the 17 August 1999 Izmit earthquake on seismic hazards in Istanbul. The 1999 Izmit and Duzce Earthquakes: Preliminary results. A. Barka, O. Kozaci, S. Akyuz and E. Altunel. Istanbul, Istanbul Tech. Univ. Press: 295-310.

Introduction

The 17 August 1999 **M**=7.4 Izmit and 12 November 1999 **M**=7.1 Düzce earthquakes killed 18,000 people, destroyed 15,400 buildings, and caused $10-25 billion in damage. But the Izmit event is only the most recent in a largely westward progression of seven large earthquakes along the North Anatolian fault since 1939. Just northwest of the region strongly shaken in 1999 lies Istanbul, a rapidly growing city that has been heavily damaged by earthquakes twelve times during the past 15 centuries. Here we calculate the probability of future earthquake shaking in Istanbul using new concepts of earthquake interaction, in which the long-term renewal of stress on faults is perturbed by transfer of stress from nearby events.

Stress triggering has been invoked to explain the 60-year sequence of earthquakes rupturing toward Istanbul (e.g., Ketin, 1969, Barka, 1996, Toksoz et al., 1979), in which all but one event promoted the next (Stein et al., 1997). Although an earthquake drops the average stress on the fault that slipped, it also changes the stress elsewhere. The seismicity rate has been observed to rise in regions of stress increase and fall where the off-fault stress decreases (e.g., Harris, 1998; Stein, 1999). The **M**=7.4 Izmit earthquake, as well as most background seismicity (Ito et al., 1999), occurred where the failure stress is calculated to have increased 1-2 bars (0.1-0.2 MPa) by **M**≥6.5 earthquakes since 1939 (Figure 1a). The Izmit event, in turn, increased the stress beyond the east end of the rupture by 1-2 bars, where the **M**=7.2 Düzce earthquake struck, and by 0.5-5.0 bars beyond the west end of the 17 August rupture, where a cluster of aftershocks occurred (Figure 1b). The correspondence seen here between calculated stress changes and the occurrence of large and small earthquakes, also reported by Hubert-Ferrari et al, (2000), strengthens the rationale for incorporating stress transfer into a seismic hazard assessment.

Methods

Dislocation calculations simulate static earthquake slip in an elastic half-space; the earthquake-induced stress changes are applied to neighboring "receiver" faults using the Coulomb failure criterion

$$\Delta CF \equiv \left|\Delta \bar{\tau}_f\right| + \mu(\Delta\sigma_n + \Delta p) \quad (1)$$

where $\Delta \bar{\tau}_f$ is the change in shear stress on a receiver fault, μ is the coefficient of friction, $\Delta \sigma_n$ is the change in normal stress acting on the receiver fault, and Δp is pore pressure change. Since a change in the Coulomb failure stress is calculated, μ on the receiver faults is treated as a constant, and is assumed not to change as a result of slip on the rupture plane. Commonly, Skempton's coefficient B_k (which varies from 0 to 1) is used to incorporate pore fluid effects, in which the effective coefficient of friction

$$\mu' = \mu(1 - B_k) \quad (2)$$

is adjusted and used in the Coulomb failure criterion as

$$\Delta CF \equiv \Delta\left|\bar{\tau}_f\right| + \mu' (\Delta\sigma_n) \quad (3)$$

after Rice, (1992).

We used a slip model for the Izmit earthquake developed from InSAR (radar satellite interferometry) (Wright et al., 1999); slip models of other earthquakes are from Nalbant et al., (1998) and Stein et al. (1997). Here the assumed friction coefficient is 0.2, as has been found for strike-slip faults with large cumulative slip (Reasenberg and Simpson, 1992; Parsons et al., 1999). A 100-bar deviatoric tectonic stress with compression oriented N55°W (Gürbüz et al., 2000) is used for map-views like in Figure 1, under which optimally oriented right-lateral faults strike E-W except along the rupture surface. To resolve stress on individual fault planes we used the program, DLC, written by R. Simpson (based on the subroutines of Okada (1992)) to calculate changes in the stress tensor at points along a specified receiver fault surface caused by slip on a source fault in an elastic half space. For resolved stresses, no tectonic stress is applied

A transient increase or decrease in the expected rate of earthquakes may occur on a fault as a consequence of slip acceleration caused by a stress change. This has been observed in the laboratory (e.g., Dieterich, 1994) and in nature (Figure 2), where a

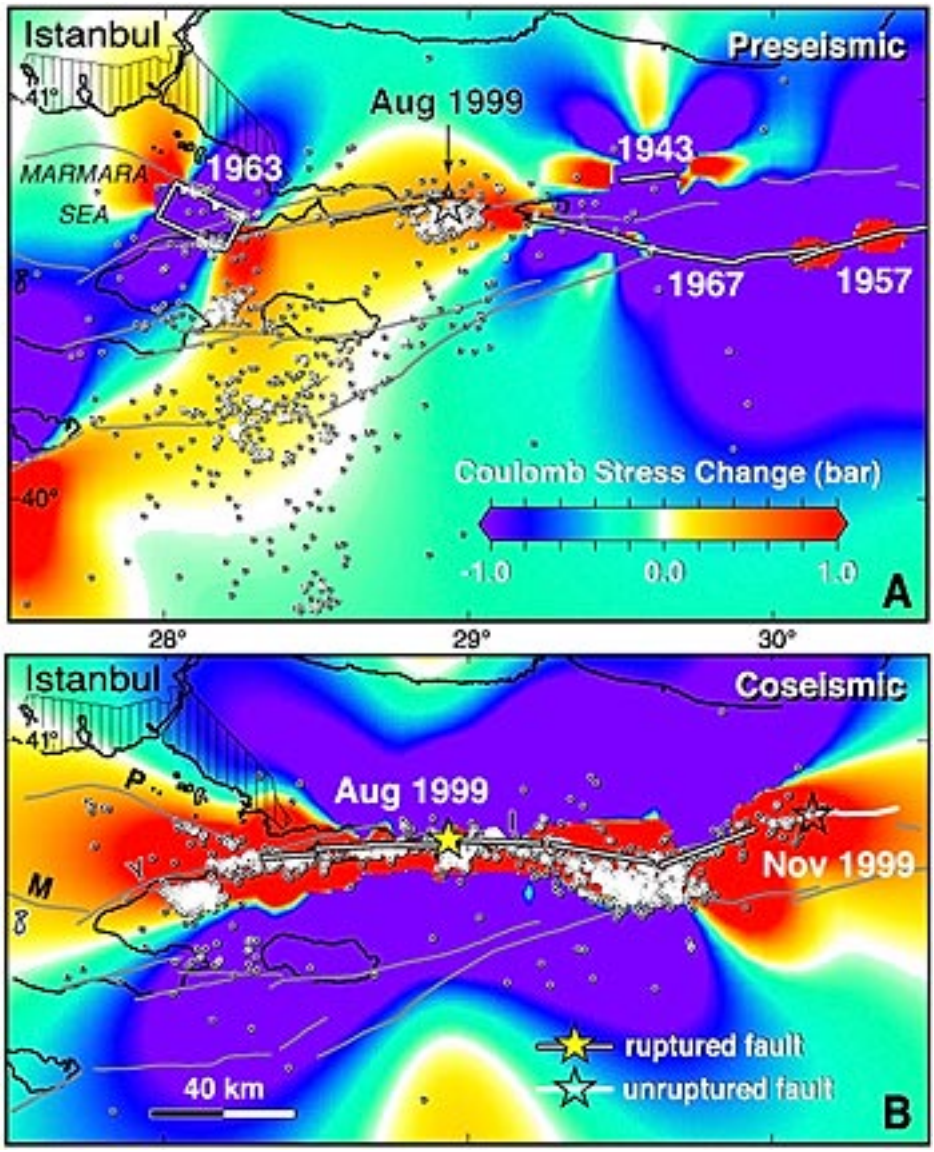

Fig. 1. (a) Stress change caused by earthquakes since 1900. Shown are the maximum Coulomb stress changes between 0 and 20 km depth on optimally-oriented vertical strike-slip faults (Harris, 1998; King et al., 1994). Seismicity recorded since installation of IZINET (1993-July 1999 (Ito et al., 1999)) has uniform coverage over the region shown. Calculated stress increases are associated with heightened seismicity rates and with the future epicenter of the 17 August 1999 Izmit earthquake; sites of decreased stress exhibit low seismicity. Before the 1999 event, two studies (Stein et al., 1997; Nalbant et al., 1998) identified this site as having increased stress and thus hazard. (b) Izmit aftershocks are associated with stress increases caused by the main rupture (first 12 days from IZINET (Ito et al., 1999)), such as the Yalova cluster southeast of "Y," and the occurrence of the 12 November Düzce earthquake. Faults: Y-Yalova, P-Prince's Islands, M-Marmara, I-Izmit.

transient decay of both large and smaller earthquakes is observed after stress perturbations. The theoretical description of the transient gain that we apply is an effect of rate- and state-dependent friction (Dieterich, 1994; Dieterich and Kilgore, 1996),

which describes behavior seen in laboratory experiments and in natural seismic phenomena, such as earthquake sequences, clustering, and the occurrence of aftershocks. The rate/state transient is predicated on the possibility that a single fault plane may have varying nucleation conditions along it, or that multiple, parallel slip planes comprise the fault zone. The transient effect assesses the possibility of nucleation (or suppression of nucleation) by a patch during the acceleration resulting from a stress perturbation.

Dieterich (1994) derived a time-dependent seismicity rate R(t), after a stress perturbation as

$$R(t) = \frac{r}{\left[\exp\left(\frac{-\Delta\tau}{a\sigma}\right) - 1\right]\exp\left[\frac{-t}{t_a}\right] + 1} \qquad (4)$$

where r is the steady-state seismicity rate, $\Delta\tau$ is the stress step, σ is the normal stress, and t_a is an observed aftershock duration, a fault-specific parameter. An example application of this concept is to earthquake clustering and aftershocks, where R(t) takes the form of Omori's law.

The transient change in expected earthquake rate R(t) after a stress step can be related to the probability of an earthquake of a given size over the time interval Δt through a nonstationary Poisson process as

$$P(t,\Delta t) = 1 - \exp\left[-\int_t^{t+\Delta t} R(t)dt\right] = 1 - \exp(-N(t)), \qquad (5)$$

after Dieterich and Kilgore (1996), where N(t) is the expected number of earthquakes in the interval Δt. This transient probability change is superimposed on the permanent change that results from a time shift, or a change in the repeat time as discussed previously. Integrating for N(t) yields

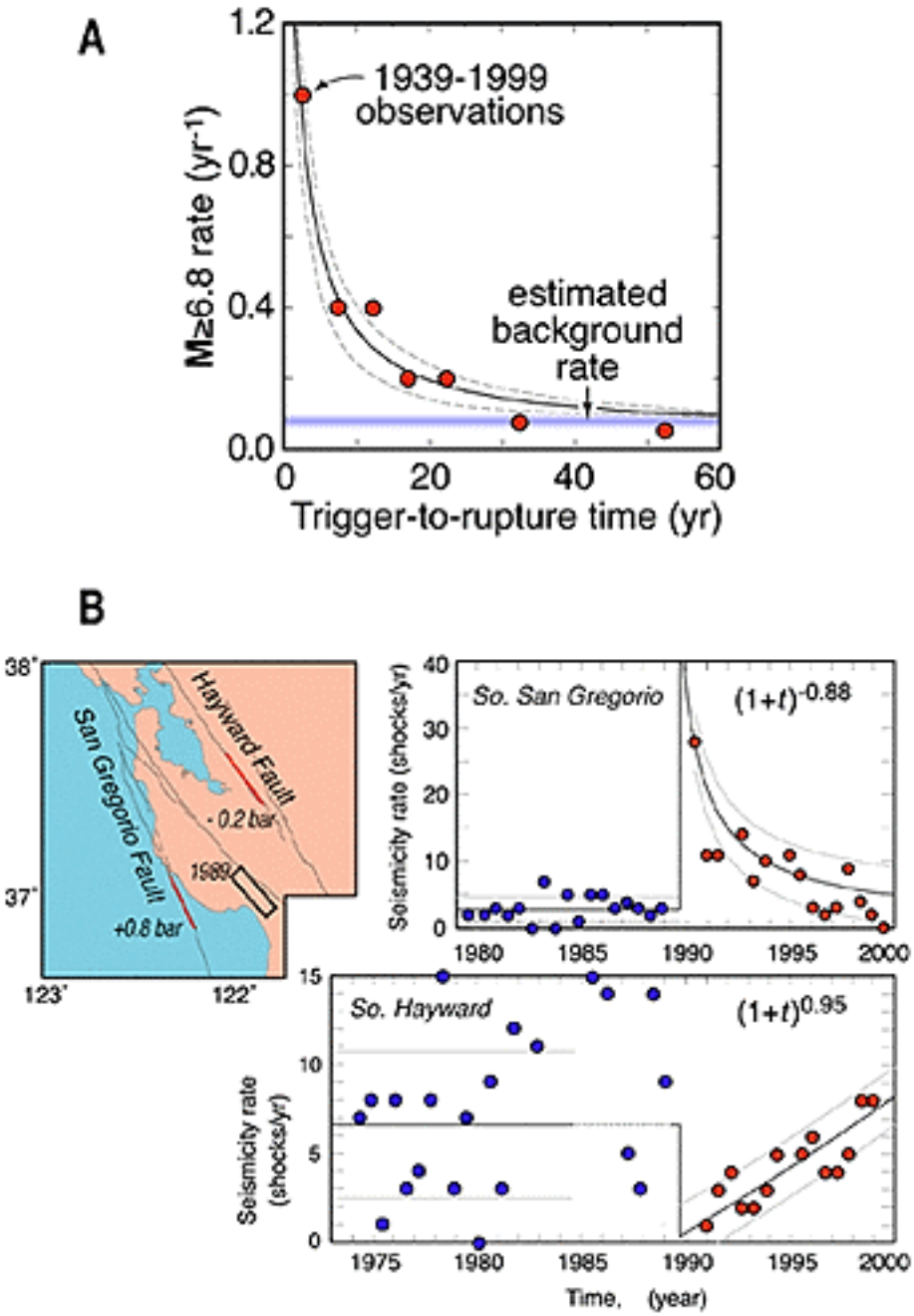

Fig. 2. (a) Transient response to stress transfer. The thirteen **M**≥6.8 North Anatolian earthquakes for which the stress at the future epicenter was increased by ≥0.5 bars are plotted as a function of time. The earthquake rate decays as t^{-1} in a manner identical to aftershocks, as predicted by (Dieterich, 1994). (b) Seismicity rate changes after the 1989 M=7.1 Loma Prieta earthquake for the San Gregorio, and Hayward faults. Even though these earthquakes occurred outside of the 'aftershock zone', the decay rates are fit to an Omori law curve. The southern Hayward fault shows a gradual seismicity rate recovery from a relaxing stress caused by the Loma Prieta quake, and can be fit to an 'inverse' Omori trend.

$$N(t) = r_p \left\{ \Delta t + t_a \ln \left[\frac{1 + \left[\exp\left(\frac{-\Delta\tau}{a\sigma}\right) - 1 \right] \exp\left[\frac{-\Delta t}{t_a}\right]}{\exp\left(\frac{-\Delta\tau}{a\sigma}\right)} \right] \right\} \quad (6)$$

where r_p is the expected rate of earthquakes associated with the permanent probability change. This rate can be determined by again applying a stationary Poisson probability expression as

$$r_p = \left(-1/\Delta t\right) \ln\left(1 - P_c\right) \quad (7)$$

where P_c is a conditional probability, and can be calculated using any distribution. We use two distributions: Brownian Passage Time here (Matthews, submitted, 2000) which has a density function

$$f(t,\mu,\alpha) = \left(\frac{\mu}{2\pi\alpha^2 t^3} \right) \exp\left(\frac{\left(t-\mu\right)^2}{2\pi\alpha^2 t} \right), \quad (8)$$

where μ is the average repeat time and α is the aperiodicity, equivalent to the coefficient of variation, and a lognormal distribution (e.g., Working Group on California Earthquake Probabilities, 1990). No catalog is adequate to estimate the coefficient of variation of the inter-event time, so we use a conservative value of 0.5 (e.g., Ogata, 1999; Working Group on California Earthquake Probabilities, 1999). In addition to the inter-event time and elapsed time on each fault, this technique requires values for the stress change on each fault (we use the average calculated stress change resolved on each fault surface), the transient decay (shown in Figure 2) from data in (Barka, 1996; Stein et al., 1997)), and a stressing rate on each fault derived from the fault geometry and the observed strain rate (0.1 bar/yr) (Stein et al., 1997).

Earthquake catalog for the Sea of Marmara: AD1500-2000

A probabilistic hazard analysis is no better than the earthquake catalog on which it is based. Global observations support an earthquake renewal process in which the

probability of a future event grows as the time from the previous event increases (Ogata, 1999). To calculate such a renewal probability, ideally one wants an earthquake catalog containing several large events on each fault to deduce earthquake magnitudes, the mean inter-event time of similar events, and the elapsed time since the last shock on each fault. Although such catalogs are rarely, if ever, available, Ambraseys and Finkel compiled a wealth of earthquake damage descriptions for events since AD 1500 in the Marmara Sea region (Ambraseys and Finkel, 1990, 1991, 1995; Finkel and Ambraseys, 1996). We assigned modified Mercalli intensities (MMI) to 200 damage descriptions (Table 1), and used the method of Bakun and Wentworth (1997) to infer **M** and epicentral location from MMI through an empirical attenuation relation. The relation

$$\mathbf{M}_i=(MMI_i+3.29+0.0206d_i)/1.68, \quad (9)$$

where d_i is distance in km between intensity (MMI) observation and epicenter, was developed from 30 California shocks with both intensity and instrumental observations (Bakun and Wentworth, 1997). The RMS fit to this relation is calculated for trial locations on a 5x5 km-spaced grid. We excluded felt reports (MMI<IV) and MMI>VIII observations were saturated to VIII because criteria for higher intensities involve observations other than building damage, and because for poorly constructed, or already partly degraded masonry, damage may be total at MMI=VIII. We calibrated the relation against Marmara Sea events that have both intensity and instrumental data (Figure 3). We calibrated with the 1912 M_S=7.4 Saros-Marmara (360 intensities; (Ambraseys and Finkel, 1987)), 1963 M_S=6.4 Yalova (11 intensities; (Ambraseys, 1988)), and 1999 **M**=7.4 Izmit earthquakes (185 intensities). For the 1912 and 1999 events, we randomly selected 50 sets of 25 intensities (the mean number for the historical shocks) to calculate epicentral and magnitude errors. This yields intensity centers within ±50 km (at 95% confidence) of the instrumental epicenters, and gives the correct **M** or M_S within ±0.3 magnitude units. Site corrections were not made because we find no tendency for epicenters to be pulled toward sedimentary sites, and because improvement was only found by Bakun and Wentworth (1997) when detailed site geology was available.

Uncertainties in earthquake location were explicitly calculated from MMI inconsistencies and inadequacies.

Our catalog consists of nine **M**≥7 earthquakes in the Marmara Sea region since 1500. For the six events that occurred before instrumental recording began in 1900, we selected the minimum magnitude falling within the 95% confidence bounds at locations associated with faults of sufficient length (Parke et al., 1999) to generate the event (Figure 4). We estimated rupture lengths and the mean slip from empirical relations on **M** for continental strike-slip faults (Wells and Coppersmith, 1994). The locations and geometry of faults in the Marmara Sea are under debate; we follow (Parke et al., 1999), which is based on seismic reflection profiles (Figure 4), and find four faults capable of producing strong shaking in Istanbul: the Yalova, Izmit, Prince's Islands, and central Marmara. Our catalog suggests two earthquakes on the Izmit fault (1719,1999), yielding an inter-event time of ~280 yr, and three on the Yalova fault (1509, 1719, 1894), permitting an estimate of ~190 yr. The most recent event for the Yalova segment is 1894.6; Izmit segment, 1999.7; Ganos fault, 1912.7; Prince's Islands fault, 1766.7; central Marmara fault, 1509.8. We infer one earthquake (May 1766) on the Prince's Islands fault and one (1509) on the central Marmara fault (Figure 4). For these, we gauge inter-event times by dividing the seismic slip estimated from the catalog by the GPS-derived slip rate (Working Group on California Earthquake Probabilities, 1995; Straub et al., 1997), yielding a ~210 yr inter-event time for the Prince's Islands fault and ~540 yr for the central Marmara fault. Thus at least two of the four faults are likely late in their earthquake cycles

One way to validate the catalog magnitudes, locations, and segment inter-event times is to compare the relative abundance of small to large shocks through the b-value; another is to see if the seismic strain release from the catalog is consistent with the measured strain accumulation from GPS. The frequency-magnitude relation for our catalog yields b=1.1 by maximum likelihood (Aki, 1965), close to the global average (Wesnousky, 1999). Over a sufficiently long time period, the moment release by earthquakes must balance the moment accumulation by elastic strain if aseismic creep is

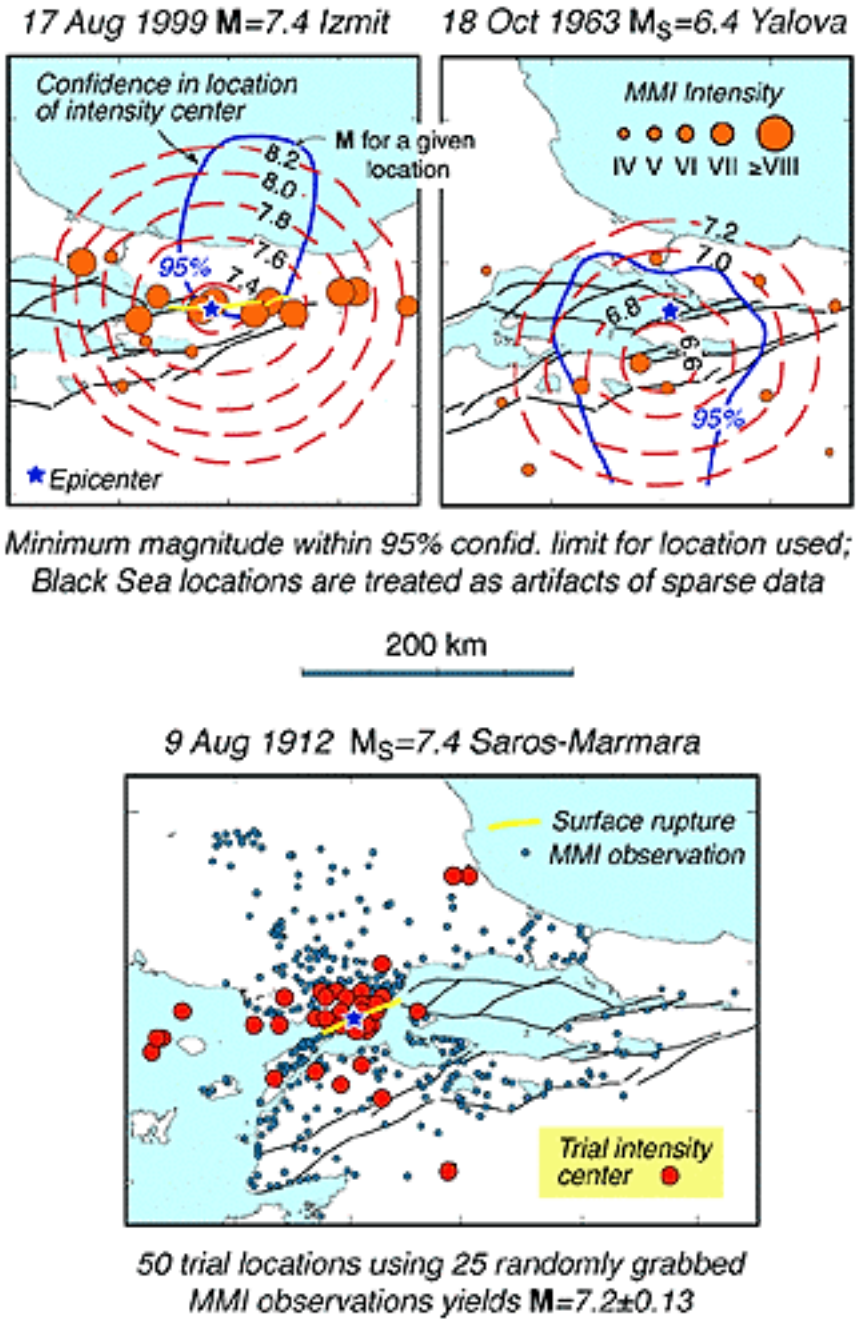

Fig. 3. We tested the technique of Bakun & Wentworth (1997) on the 1999, 1963, and 1912 Marmara Sea earthquakes (each with known locations and magnitude) to ensure that the empirical relation developed with California earthquakes can be used in Turkey and to find minimum uncertainties. For the 1912 event, we randomly selected 50 sets of 25 intensities (the mean number for the historical shocks) to calculate epicentral and magnitude errors. This yields intensity centers within ±50 km (at 95% confidence) of the instrumental epicenters, and gives the correct **M** or M_S within ±0.3 magnitude units.

negligible. We compared the seismic slip rate represented by the catalog (Includes earthquakes in 1509, 1556, 1719, 1754, 1766, 1855, 1857, 1863, 1877, 1894, 1953, and 1964 from Ambraseys and Finkel (1990, 1991, 1995) and Nalbant et al. (1998)) (23.5±8 mm/yr) to the observed slip rate measured by GPS across the North Anatolian fault system in the Marmara region (22±3 mm/yr) (quoted uncertainties are one standard deviation here and elsewhere (Straub et al., 1997) (Figure 5). For b~1, most of the moment is conferred by the largest shocks, so the consistency between GPS and catalog strain means that the size and location of the three **M**~7.6 events, as well as the number of smaller earthquakes, are plausible..

Perhaps the strongest test of the 500-yr catalog can be made by calculating the combined Poisson, or time-independent, probability predicted from the inter-event times for the three faults we regard as capable of producing MMI≥VIII shaking in Istanbul. This is the probability averaged over several earthquake cycles on each fault, and yields 29±15% in 30 yr. This can be compared to the Poisson probability calculated directly from the longer record of MMI≥VIII shaking in Istanbul during the preceding ~1000 years (AD447-1508). The older record gives the long-term frequency of shaking used in a Poisson calculation without knowledge of the earthquake locations. At least 8 earthquakes (AD 447, 478, 542, 557, 740, 869, 989, 1323) caused severe damage in Istanbul between AD 447 and 1508 (Ambraseys and Finkel, 1990, 1991, 1995), translating into a 20±10% 30-yr probability, roughly comparable to that derived from our catalog. Thus the fault inter-event times estimated from the 500-yr catalog are consistent with the independent record of shaking in Istanbul during the preceding millennium.

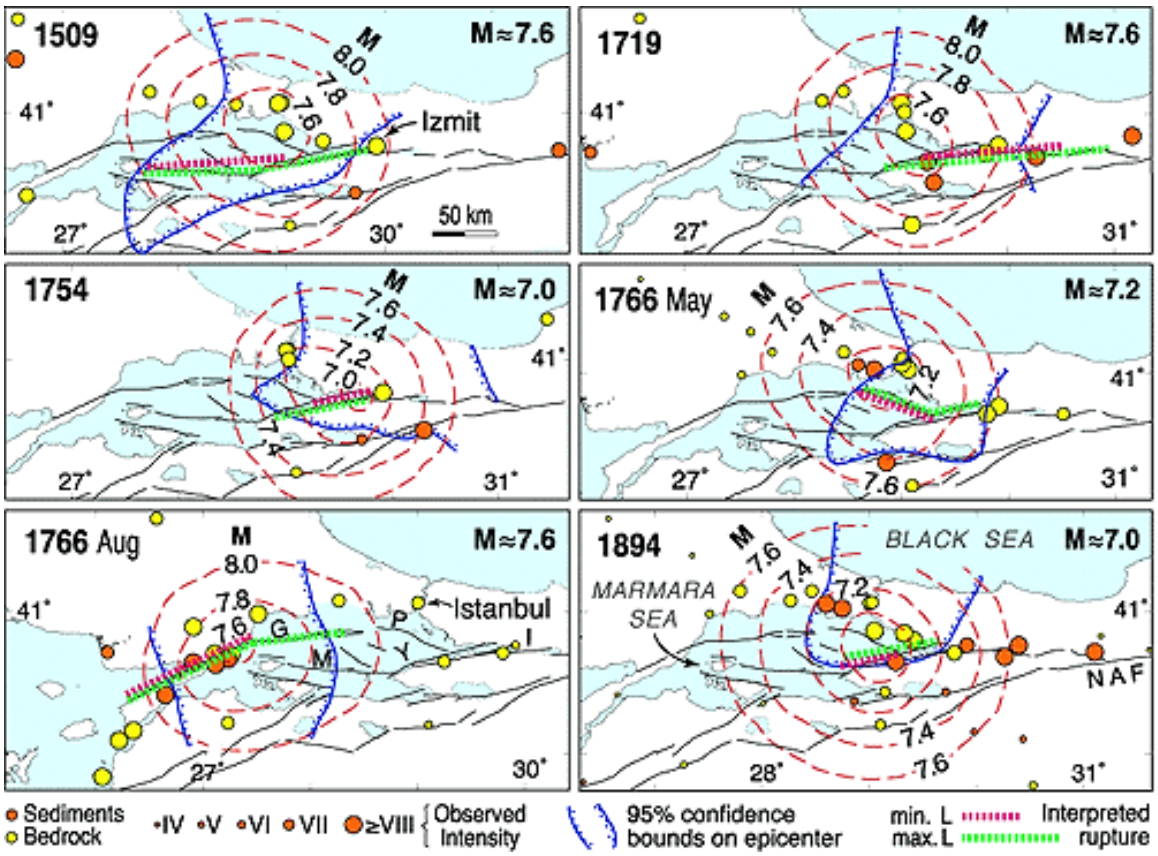

Fig. 4. Large historical earthquakes since 1500. Intensities (dots) were assigned from damage descriptions compiled by (Ambraseys and Finkel, 1990, 1991, 1995; Finkel and Ambraseys, 1996). Red dashed contours give the moment magnitude **M** needed to satisfy the observations for a given location (Bakun and Wentworth, 1997), because the farther the epicenter is from the observations, the larger the **M** required to satisfy them. The confidence on location is governed by the relative intensities; magnitude is a function of absolute intensities. We assigned earthquakes to faults by minimizing **M** within the 95% confidence region (see text for further detail). Faults labeled in lower panels: I-Izmit, Y-Yalova, P-Prince's Islands, M-Marmara, G-Ganos, NAF-North Anatolia fault.

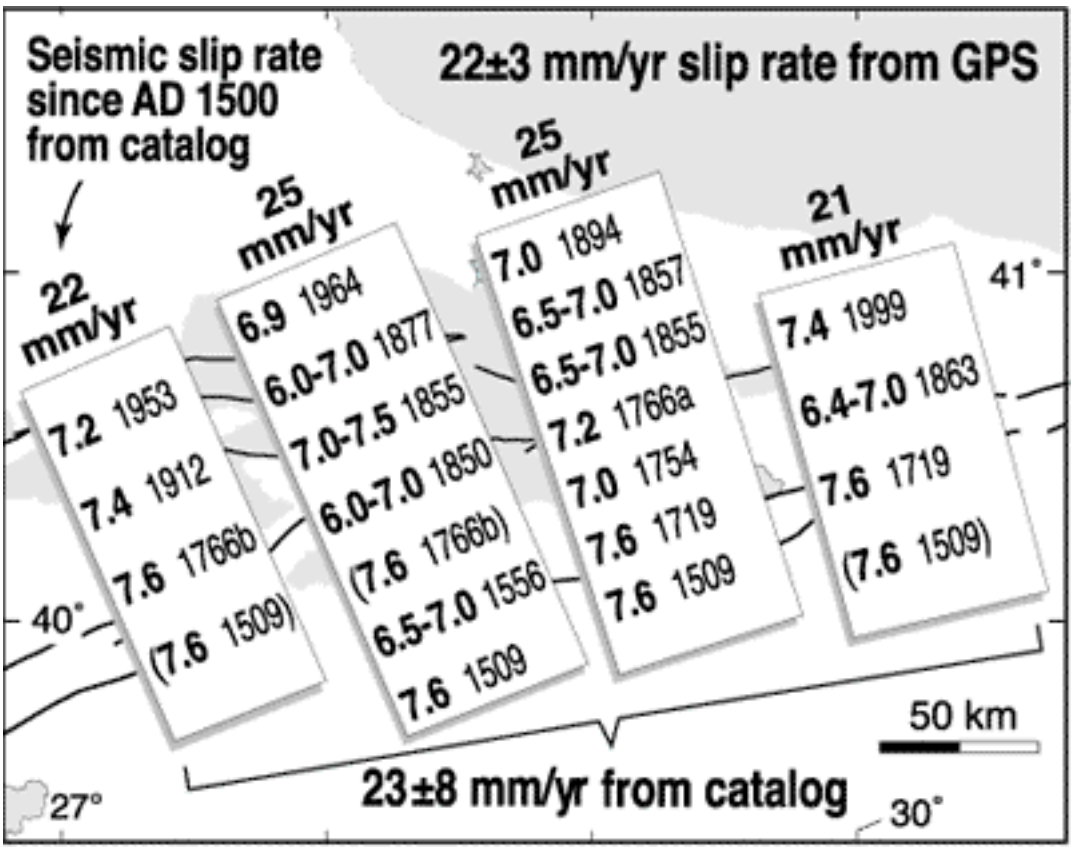

Fig. 5. Seismic slip from the 500-yr-long catalog of Fig. 2 is summed in four transects across the North Anatolia fault system in the Marmara Sea. All known or estimated **M**≥7 sources are included. The mean seismic strain release rate balances the strain accumulation rate observed from GPS geodesy (Straub et al., 1997). Whether earthquakes in parentheses extend to a given transect is uncertain. '1766a' is May; '1766b' is August.

Earthquake probability for greater Istanbul

We combined earthquake renewal and stress transfer into the probability calculation on the basis that faults with increased stress will fail sooner than unperturbed faults. Because two out of the three faults within 50 km of Istanbul are interpreted to be late in their earthquake cycles, the renewal probability is higher than the Poisson probability. Additionally, the permanent probability gain caused by stress increase is amplified by a transient gain that decays with time. We estimated the duration of the transient decay directly from the times between triggering and rupturing earthquakes on the North Anatolian fault (Figure 6a). Because parameter assignments used in the calculation are approximate, we perform a Monte Carlo simulation to explore the

uncertainties by making 1000 probability calculations to establish error bounds (Savage, 1991). Four parameters (stress change, stressing rate, transient duration, and inter-event time) for the Monte Carlo simulations are drawn at random from a normal distribution with a shape factor of 0.25 about each estimate, except for the inter-event time for which the shape factor is 0.5. Alternating Monte Carlo trials were run with a Brownian passage time and lognormal distribution. We combine the probability of multiple faults with the expression

$$P=1-(1-P_a)(1-P_b)(1-P_c) \quad (10)$$

for faults a-c. This method assumes independent sources of hazard, since we cannot include future interactions and for all but the most recent earthquakes, we cannot include past interactions.

The probability functions we generate (Figure 6b) exhibit a gradual rise as the mean time since the last shock on each fault grows, and a sharp jump in August 1999 followed by a decay. We find a 62±15% probability of strong shaking (MMI≳VIII; equivalent to a peak ground acceleration of 0.34-0.65g (Wald et al., 1999)) in greater Istanbul over the next 30 yr (May 2000-2030), 50±13% over the next 22 yr, and 32±12% over the next 10 yr (Table 2). Inclusion of renewal doubles the time-averaged probability; interaction further increases the probability by a factor of 1.3..

The twelve earthquakes that damaged Istanbul during the past 1500 yr attest to a significant hazard, and form the basis for a 30-yr Poisson, or time-averaged, probability of 15-25%. Because the major faults near Istanbul are likely late in their earthquake cycles (with no major shocks since 1894), the renewal probability climbs to 49±15%. We calculate that stress changes altered the rate of seismicity after the 1999 Izmit earthquake, promoting the **M**=7.2 Düzce shock and the Yalova cluster. Because the 1999 Izmit shock is calculated to have similarly increased stress on faults beneath the Marmara Sea, the interaction-based probability we advocate climbs still higher, to 62±15%.

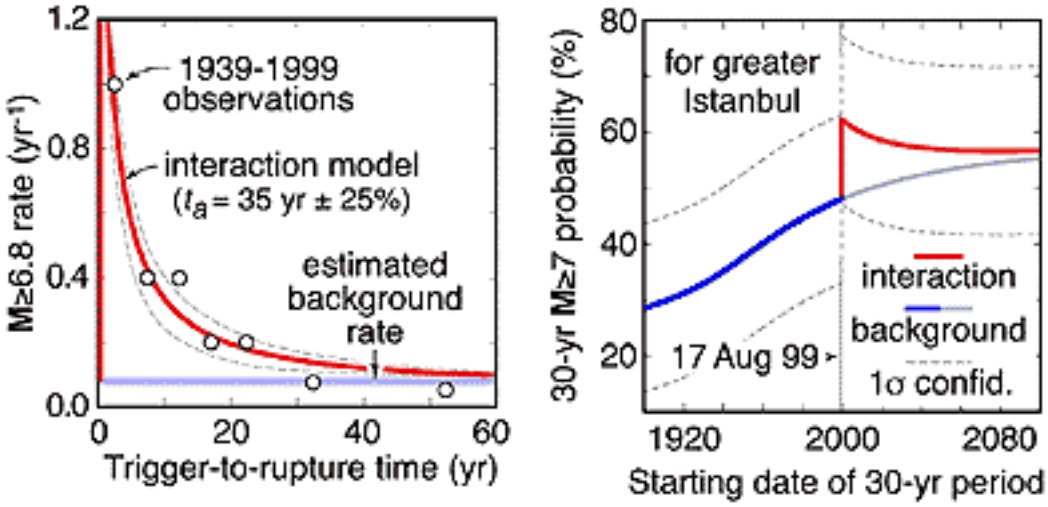

Fig. 6. The North Anatolian fault observations from Figure 2 are shown fit to a transient curve calculated with Dieterich's (1994) method fit to a 35-yr transient decay. Below, the calculated probability of a **M**≥7 earthquake (equivalent to MMI≳VIII shaking in greater Istanbul) is shown as a function of time. The probability on each of three faults is summed using equation 10. The large but decaying probability increase is caused by the 17 August 1999 Izmit earthquake. 'Background' tracks the probability from earthquake renewal; 'interaction' includes renewal and stress transfer. Light blue curve gives the probability had the Izmit earthquake not occurred.

Acknowledgments

We thank N. Ambraseys, T. Wright, E. Fielding, A. Ito, J. Parke, and C. Finkel for sharing their insights and preliminary results with us, W. Bakun for his code and his review, and J. C. Savage, and W. Thatcher, C. Straub, and S. Kriesch for incisive reviews. Support from SwissRe is gratefully acknowledged.

References

Aki, K., 1965. Maximum likelihood estimate of *b* in the formula log N=*a*-*b*M and its confidence limits. Bull. Earthquake Res. Ins. 43, 237-239.

Ambraseys, N. N., Finkel, C. F., 1987. Seismicity of Turkey and neighboring regions, 1899-1915. Annales Geophysicae 5, 701-725.

Ambraseys, N. N., 1988. Engineering seismology. Earthqu. Engin. and Structural Dynamics 17, 1-105.

Ambraseys, N.N., Finkel, C. F. 1990. The Marmara sea earthquake of 1509. Terra Nova 2, 167-174.

Ambraseys, N. N., Finkel, C. F., 1991. Long-term seismicity of Istanbul and the Marmara sea region, Terra Nova 3, 527-539.

Ambraseys, N. N., Finkel, C. F., 1995. The Seismicity of Turkey and Adjacent Areas: A historical review, 1500-1800. Muhittin Salih EREN, Istanbul.

Bakun, W. H., Wentworth, C. M., 1997. Estimating earthquake location and magnitude from seismic intensity data. Bull. Seismol. Soc. Amer. 87, 1502-1521.

Barka, A. A., 1996. Slip distribution along the North Anatolian fault associated with large earthquakes of the period 1939 to1967. Bull. Seismol. Soc. Am. 86, 1238-1234.

Dieterich, J. H., 1994. A constitutive law for rate of earthquake production and its application to earthquake clustering. J. Geophys. Res. 99, 2601-2618.

Dieterich, J. H., Kilgore, B., 1996. Implications of fault constitutive properties for earthquake prediction. Proc. Nat. Acad. of Sci. USA 93, 3787-3794.

Finkel, C. F., Ambraseys, N. N., 1996. The Marmara Sea earthquake of 10 July 1894 and its effect on historic buildings, Anatolia Moderna Yeni Anadolu VII (Bibliothèque de l'Institut Français d'Etudes Anatoliennes-Georges Dumézil, Paris), 43.

Gürbüz, C., Aktar M., Eyidogan, H., Cisternas, A., Haessler, H., Barka, A., Ergin, M., Turkelli, N., Polat, O., Ucer, S. B., Kuleli, S., Baris, S., Kaypak, B., Bekler, T., Zor, E., Bicman, F., Yoruk, A., 2000. The seismotectonics of the Marmara Region (Turkey): Results from a microseismic experiment. Tectonophysics 316, 1-17.

Harris, R. A. , 1998. Introduction to special session: Stress triggers, stress shadows, and implications for seismic hazard. J. Geophys. Res. 103, 24347-24358.

Hubert-Ferrari, A., Barka, A., Jaques, E., Nalbant, S. S., Meyer, B., Armijo, R., Tapponnier, P., King, G. C. P., 2000. Seismic hazard in the Marmara Sea region following the 17 August 1999 Izmit earthquake. Nature 404, 269-273.

Ito, A., et al., 1999. Precise Distribution of Aftershocks of the Izmit Earthquake of August 17, 1999, Turkey. Eos Trans. 80, F662 (1999).

Ketin, I., 1969. Uber die nordanatolische Horizontalverschiebung. Bull. Min. Res. Explor. Inst. Turkey 72, 1-28.

King, G. C. P., R. S. Stein, J. Lin, 1994. Static stress changes and the triggering of earthquakes, Bull. Seismol. Soc. Amer. 84, 935-953.

Nalbant, S. S., A. Hubert, G. C. P. King, J. 1998. Stress coupling between earthquakes in northwest Turkey and the north Aegean Sea. J. Geophys. Res, 103, 24469-24486.

Ogata, Y., 1999. Estimating the hazard of rupture using uncertain occurrence times of paleoearthquakes, J. Geophys. Res. 104, 17995-18014.

Okada, Y., 1992. Internal deformation due to shear and tensile faults in a half-space, Bull. Seismol. Soc. Am. 82, 1018-1040.

Parke, J. R., Minshull, T. A., Anderson, G., White, R. S., McKenzie, D., Kuscu, I., Bull, J. M., Gorur, N., Sengor, C., 1999. Active faults in the Sea of Marmara, western Turkey, imaged by seismic reflection profiles. Terra Nova, 11, 223-227.

Parsons, T., Stein, R. S., Simpson, R. W., Reasenberg, P. A., 1999. Stress sensitivity of fault seismicity: A comparison between limited-offset oblique and major strike-slip faults. J. Geophys. Res. 104, 20183-20202.

Reasenberg, P. A., R. W. Simpson, 1992. Response of regional seismicity to the static stress change produced by the Loma Prieta earthquake. Science 255, 1687-1690.

Savage, J. C., 1991. Criticism of some forecasts of the National Earthquake Prediction Evaluation Council. Bull. Seismol. Soc. Am. 81, 862-881.

Stein, R. S., 1999. The role of stress transfer in earthquake occurrence, Nature 402, 605-609.

Stein, R. S., Barka, A. A., Dieterich, J. H., 1997. Progressive failure on the North Anatolian fault since 1939 by earthquake stress triggering. Geophys. J. Int. 128, 594-604.

Straub, C., Kahle, H.-G., Schindler, C., 1997. GPS and geological estimates of the tectonic activity in the Marmara Sea region, NW Anatolia, J. Geophys. Res. 102, 27587-27601.

Toksoz, M. N., Shakal, A. F., Michael, A. J., 1979. Space-time migration of earthquakes along the North Anatolian fault zone and seismic gaps. Pageoph 117, 1258-1270.

Wald, D. J., V. Quitoriano, T. H. Heaton, H. Kanamori, 1999. Relationships between peak ground acceleration, peak ground velocity, and modified Mercalli intensity in California. Earthquake Spectra 15, 557-564.

Wells, D. L., Coppersmith, K. J., 1994. New empirical relationships among magnitude, rupture length, rupture width, rupture area, and surface displacement. Bull. Seismol. Soc. Amer. 84, 974-1002.

Wesnousky, S. G., 1999. Crustal deformation processes and the stability of the Gutenberg-Richter relationship. Bull. Seismol. Soc. Amer. 89, 1131-1137.

Working Group Calif. Earthquake Probabilities, 1995. Seismic hazards in southern California: Probable earthquakes, 1994-2014. Bull. Seismol. Soc. Amer. 85, 379-439.

Wright, T. J., England, P. C., Fielding, E. J., Haynes, M., Parsons, B. E., 1999. Eos Trans. 80, F671

Matthews, M. V., 2000. A stochastic model for recurrent earthquakes, J. Geophys. Res. submitted.

Working Group Calif. Earthquake Probabilities, 1990. Probabilities of large earthquakes in the San Francisco Bay region, California, *U. S. Geol. Surv. Circ., 1053*, 51pp.,

Working Group Calif. Earthquake Probabilities, 1999. Probabilities of large earthquakes in the San Francisco Bay region, California, U. S. Geol. Surv. Open File Rep. 99-517

Table 1. Modified Mercalli Intensity assignmnets form damage descriptions compiled by Ambraseys and Finkel [1990, 1991, 1995].

Note: MMI Roman numerals listed as numbers; half units average a range

Earthquake		**1509**	**1719**	**1754**	**1766**a	**1766**b	**1894**	**1912**	**1999**
date		10-Sep	25-May	2-Sep	22-May	5-Aug	10-Jul	9-Aug	29-Sep
Notes		*4*					*1*	*3*	*2*
Reported deaths		>5000*	6000	2000	5300	>5000	1300	>2000	30,000
Major tsunami		Izmit bay			Izmit bay				
# observations		19	18	11	19	30	43	26	19
Site Name	**Soft seds**								
Adapazari	Y						8		9
Akyazi	Y								8.5
Ankara	N			3			3		3
Avlonya	N						3		
Aydin	Y					3	3		
Aytos	N				3				
Balkans	N					3			
Bandirma	N						5.5		
Bilecik	N						5.5		
Bolu	Y	7.5					4	3	7
Bosphorous	N	7.5		7.5	8		7		6
Bozcaada	N				3.5	8	3		
Bucharest	Y						3	3	
Burdur	Y						3		
Bursa	N	6.5	8	6.5	7	6	6.5	5	6
Büyükçakmece	Y	7			7		8		
Cairo	Y	3							
Çanakkale	Y					8		8	
Çatalca	N		7		7		7		
Chalkis (Greece)	N						3		
Çorlu	N	7			6		7	7	
Danube basin	Y	3				3			
Dimetoka	Y	8.5							
Düzce	Y		9.5				4		8
Edirne	N	7	6.5	4	5	7	5	6	
Edremit	Y							6	
Enez	Y		7			7		8	
Eregli	N			7					
Eskisehir	Y						6		4
Evrese	Y					8.5			

Ezine	Y						4		
Galata/Pera	N				8				
Gazikoy	Y					9	5	9	
Gebze	N	8.5					8		7.5
Gelibolu	N	7.5				9	5	9	
Gemlik	Y						6.5		
Geyve	Y			8.5					
Golyaka	Y								9
Gülcük (on fault)	Y					9			9.5
Hora	Y					9.5			
Imroz	N							8	
Istanbul	N	9	8	7.5	8.5	7	7.25	6	6
Izmir	Y		4	4	3	3		3	
Izmit	N	9	9.5	8	8.5	6	7.5	5	8.5
Iznik	Y	7		6.5			6	5	6
Karamürsel	N		9.5		8	7	7.5		8
Karisdiran	N				6			7	
Kartel/Pendik	N						8		
Kilidbahir	N					8			
Konya	Y						3		
Korfez	Y								8
Küçükçekmece	Y				8		8		8
Lüleburgaz	N				6		5	7	
Malkara	N					8			
Mitilini	N					7			
Mt. Athos	N	3	3			3			
Mudanya	Y				8		6		
Mudunru	Y						4		
Mürefte	Y					9		9	
Mustafakemalpasa	Y						4		
Orhangazi	Y		8.5						6
Princess Is	N	8	7.5				8		
Sapanca	Y		9.5				9		8
Sarkoy	Y					9		9	
Seddulbahir	N					8		8	
Siebenburg	N	3							
Silivri	N	7					7		
Silivri (N. of)	N		7						
Sofia (Bulgaria)	Y						3	3	
Sopron	N					3			
Tanem	N	3							
Tekirdag	N				6	8.5	6	8	
Thasos	N							6	
Thessaloniki	Y		4		3	3		3	
Üsküdar	N		7.5	7.5					
Vienna	Y					3			

Yalova	Y		10			7	8.5	5	8
Yannina (Iannina)	Y						3		
Yenice	Y						5.5		
Yesilkoy/St Stephano	Y						7.5		

Bursa, Erdine, Istanbul, Izmit reported for all shocks: Double their weight as references?
Coverage uniformly poor south of Marmara Sea

NOTES

1 Finkel & Ambraseys supplemented by D. Eginitis, Le tremblement de terre de Constantinople Annales de Géographie, 4, 151-165 (1895).

2 1999 MMI based on Barka's 3 flights & field visits, with calibaration against RMS MMI maps; du 10 juillet 1894, Turkish General Directorate MMI map ignored as inflated.

3 Assignments tentative; we're missing a key figure from A & F (1987)

4 Eginitis (1895) gives 13,000 deaths

Table 2. Earthquake probabilities for faults within 50 km of Istanbul beginning May 2000. 'Combined' is the probability for the three faults. Quoted uncertainties are one standard deviation. 'Background' refers to renewal; 'interaction' includes renewal and interaction by stress transfer.

Fault	**30 Year (%)**		**10 Year (%)**		**1 Year (%)**	
	Interaction	Background	Interaction	Background	Interaction	Background
Yalova	33±21	22±18	14±11	7±7	1.7±1.7	0.8±0.8
Prince's Is.	35±15	26±12	16±9	10±6	2.1±1.6	1.1±0.7
Marmara	13±9	11±8	5±5	4±4	0.6±0.7	0.5±1.0
Combined	62±15	49±15	32±12	20±9	4.4±2.4	2.3±1.5